

**Measurements of PVT_x and Saturation Properties
for the Binary 1,1,1,2-Tetrafluoroethane + Propane System¹**

Satoshi Naganuma,² Atsuhiko Mizote,² and Koichi Watanabe^{2,3}

¹ Paper presented at the Fourteenth Symposium on Thermophysical Properties, June 25-30, 2000, Boulder, Colorado, U.S.A.

² Department of System Design Engineering, Faculty of Science and Technology, Keio University, 3-14-1, Hiyoshi, Kohoku-ku, Yokohama, 223-8522, Japan.

³ To whom correspondence should be addressed.

Abstract

Natural refrigerants such as hydrocarbons (HCs) are considered being promising long-term alternatives in some of the restricted applications for refrigeration systems, since they have zero ODP values and negligible GWP values. One of the crucial disadvantages of HCs, however, is flammability. For the purpose of solving this important issue, we have challenged to study on the thermodynamic properties of binary mixtures of HC blended with nonflammable HFC refrigerant. The present paper, therefore, aims to measure a set of reliable PVT_x property data for the binary 1,1,1,2-tetrafluoroethane (R-134a) + propane (R-290) mixtures in two-phase and gas-phase regions. The experimental PVT_x properties of the binary R-134a + R-290 system have been measured at four different compositions by a constant-volume method coupled with expansion procedures in an extensive range of temperatures from 312 K to 400 K, pressures up to 6.1 MPa and densities up to $196 \text{ kg}\cdot\text{m}^{-3}$, respectively. The present study also aims to determine the dew-point pressures and the saturated-vapor densities of the present binary mixtures so as to develop a virial equation of state in the gaseous phase of the binary R-134a + R-290 system.

KEY WORDS: binary refrigerant mixtures; constant-volume method; dew-point pressure; natural working fluid; propane; R-134a; saturated vapor density.

Introduction

The refrigeration-based industries are currently facing various challenges particularly for the global environmental issues. In industrialized nations, it is believed that the hydrofluorocarbon (HFC) refrigerants and their binary or ternary mixtures are the promising alternative refrigerants to replace the banned chlorofluorocarbon (CFC) refrigerants and hydrochlorofluorocarbon (HCFC) refrigerants which are also expected to be phased out by the year 2030 under the existing international regulations. Immediately after the agreement achieved under the 1997 Kyoto Protocol of the United Nations Intergovernmental Framework Convention on Climate Change, however, the HFC refrigerants were also included among the so-called basket of greenhouse gases that should be controlled to be emitted to the atmosphere from the refrigeration and air-conditioning equipment due to their considerable impacts on the global warming.

In accord with this sort of worldwide increasing concerns about the global warming, several natural refrigerants including hydrocarbons which all are benign environmentally are recently being considered attractive to be applied for some limited applications in refrigeration and related equipment. However, an existing flammability issue regarding hydrocarbons in particular is a significant disadvantage in any proposed applications. In the present study, therefore, we aimed to propose a blend of propane, R-290, with nonflammable HFC refrigerant, 1,1,1,2-tetrafluoroethane, R-134a, since a considerable reduction both in global warming impact and flammability would be expected by this blended mixture.

Since there has been reported a few measurements of the essential thermodynamic properties of this mixture, a series of *PVTx* property measurements to cover a wide

range of compositions have been conducted in the present study. The present measurements cover the range of temperatures from 312 to 400 K, pressures up to 6.1 MPa, and densities up to $196 \text{ kg}\cdot\text{m}^{-3}$, respectively.

Experimental

A constant-mass method coupled with expansion procedures was used for the present *PVTx* property measurements of the binary R-134a (1) + R-290 (2) system. The experimental apparatus has been successfully applied by the present authors to a series of *PVTx* property measurements of the binary and/or ternary HFC refrigerants for the last several years. (Sato *et al.*¹, Kiyoura *et al.*², Uchida *et al.*³, Mizote *et al.*⁴).

The apparatus shown in Figure 1 consists of three major subsystems; a cell system, a temperature control/measuring subsystem and a pressure control/measuring subsystem, respectively.

The cell system consists of a sample cell (A), an expansion cell (B), and small-bore tubes with high-pressure valves (V1, V2, V3) and joints (J1, J2) that connect these cells with a diaphragm-type differential pressure detector (M). The sample and expansion cells are thick-walled spherical vessels made of stainless-steel and their inner volumes were carefully calibrated with pure water; they were $283.368 \pm 0.027 \text{ cm}^3$ and $55.583 \pm 0.007 \text{ cm}^3$, respectively, at 273.15 K. Similarly calibrated inner volume of the connecting tube mentioned above was $17.092 \pm 0.007 \text{ cm}^3$ at 273.15 K.

The entire cell system is kept immersed in a thermostated fluid bath (L) which is filled with silicone oil. A standard $25 \text{ } \Omega$ platinum resistance thermometer (G) calibrated against ITS-90 is used both for the detection and measurement of a fluid

temperature with an aid of a temperature bridge (H) associated by a PID controller (I). The sample pressure in the cell system is transferred through the differential pressure detector (M) to pressure transferring gas, nitrogen, whose pressure is measured by a digital quartz pressure transducer (Q) as shown in Figure 1.

A sample of the mixture is prepared as follows: pure components were carefully filled in the independent vessels which were evacuated in advance. The mass of the pure component in each vessel was adjusted to the prescribed mass and weighed by a precision chemical balance. Then the pure components were charged one by one into the sample cell cooled by liquefied nitrogen. The charged mass and composition were determined by the mass difference of each vessel before and after charging the component into the sample cell.

Then the sample cell was connected as shown in Figure 1. After the space of the connecting tube between the sample cell, the expansion cell, and the differential pressure detector was evacuated, the valve V2 was closed, and the valve V1 was opened successively. The temperature in the thermostated bath filled with silicone oil was controlled within ± 2 mK. When thermal equilibrium was reached with the pressure remaining unchanged over several hours, the temperature and pressure of the sample fluid were measured.

When a series of pressure measurements along an isochore was completed, the expansion cell was evacuated, the valve V3 was closed, and the valve V2 was opened gradually to expand part of the sample fluid into the expansion cell in the single phase. Throughout the expansion procedure, the two cells were agitated by a rocking device to ensure uniform density and composition unchanged. The valve V1 was closed when the temperature and the pressure became stable. By using these procedures, the PVT_x

measurements and the isothermal expansion procedures are repeated for several isochores under the measured composition at a single charge of the sample in this work.

The mass density along the initial isochore, ρ_0 , was determined by the following equation:

$$\rho_0 = m_0 / (V_a + V_c) \quad (1)$$

where m_0 denotes the mass of the sample, V_a denotes the inner volume of the sample cell, and V_c denotes that of the connecting tube between the sample cell, the expansion cell, and the differential pressure detector. The density after the N th expansion, ρ_N , was then determined as follows:

$$\rho_N = \prod_{i=1}^N k_i m_0 / (V_a + V_c) \quad (2)$$

where k_i denotes the volume ratio defined by the following equation:

$$k_i = V_a / (V_a + V_b + V_c) \quad (3)$$

where V_b denotes the inner volume of the expansion cell. The variations of the inner volumes V_a , V_b , and V_c due to thermal expansion and pressure deformation were naturally corrected.

The experimental uncertainties of the present measurement are estimated to be within ± 7.2 mK in temperature, ± 3.0 kPa in pressure, ± 0.085 kg·m⁻³ in density, and

0.040 mol% in composition, respectively. The sample purities are 99.95 mass% for R-134a and 99.90 mass% for R-290, as determined by the chemical manufacturers. No additional purification and analysis of the samples have been conducted in the present study.

Result And Discussion

One hundred-ten PVT_x property data of the R-134a (1) + R-290 (2) system were measured along seven isochores at temperatures from 312 to 400 K, at densities from 67 to 196 kg·m⁻³, at pressures from 1.6 to 6.1 MPa, and mole fractions of the composition of R-134a, x_1 , at 0.25, 0.50, 0.60 and 0.78 mol% as tabulated in Table 1. Figure 2 shows the distribution of the measured PVT_x property data on a pressure-temperature plane, where the vapor-pressure curves are calculated from the correlations of both pure components (the correlations proposed by Piao *et al.*⁵ in accord with the critical parameters by Aoyama *et al.*⁶ for R-134a, Miyamoto and Watanabe.⁷ for R-290). It is known that the present binary mixture is a strong positive pressure azeotrope as shown in Figure 2. Since there exist a total of 52 PVT_x property measurements reported near the saturation (Holcomb *et al.*⁸), we have tried to compare the present measurements and these reported data (Holcomb *et al.*⁸) with REFPROP (ver.6.01) in Figure 3, where the relative pressure deviations of experimental data from REFPROP (ver.6.01) are given. It becomes clear from Figure 3 that the present measurements show a systematic deviation increasing up to about -5 % at lower temperatures for each composition, but only 3 data points among 52 data reported by Holcomb *et al.*⁸ are the measurements near the saturation in vapor phase that can be compared here. It is interesting to note,

however, that these 3 data points show a considerable scatter, whereas our results show a very consistent departure from the prediction given by REFPROP (ver.6.01). Namely, the deviations of the present results for the mixtures with $x_1 = 0.25$ and $x_1 = 0.78$ are found small, while the mixtures apart from the pure components deviate significantly. This fact, therefore, suggests that the prediction by REFPROP (ver.6.01) does have a room to be improved.

In this study, six dew-point pressures and saturated-vapor densities of the R-134a + R-290 system have been determined on the basis of rather detailed $PVTx$ properties measured in the vicinity of the saturation boundary as well as the thermodynamic behavior of gaseous isochores near the saturation. Figure 4 shows a typical isochore in the two-phase region correlated with the following simple relation:

$$\ln P_r = A - B/T_r \quad (4)$$

and vapor-phase isochores near the saturation correlated with the following expression:

$$Z = C + (D/T_r) + (E/T_r^2) + F \exp(1/T_r) \quad (5)$$

where P_r , T_r and Z denotes the reduced pressure, the reduced temperature, and the compressibility factor. A , B , C , D , E , and F are the numerical constants of the correlations. The $PVTx$ measurements used to determine the dew-point pressures and the saturated-vapor densities are those within 5 K below the saturation temperature for eq 4 and those within 5 K above the saturation temperature for eq 5. The pseudocritical pressure and the pseudocritical temperature for this refrigerant mixture R-134a + R-290

system are determined as follows:

$$P_c = \sum_{i=1}^2 x_i P_{c,i} \quad (6)$$

$$T_c = \sum_{i=1}^2 x_i T_{c,i} \quad (7)$$

where x_i and $T_{c,i}$ denote the mole fraction of component i in the mixture and the critical temperature of component i , and the subscript $i = 1$ is for the pure R-134a; $i = 2$ is for the pure R-290. Each correlation represents the present $PVTx$ measurements within the estimated experimental uncertainty. After determining the numerical constants, A through F, along each isochore, the dew-point pressure and saturated-vapor density were calculated with the aid of the Newton-Raphson method. Dew-point pressure and saturated-vapor density values thus determined are summarized in Table 2. Figure 5 shows the dew-point pressures on a pressure-temperature plane. The uncertainty of these values are estimated to be within ± 0.10 K in temperature, ± 4.2 kPa in pressure, and $\pm 0.12 \text{ kg} \cdot \text{m}^{-3}$ in density, respectively.

Conclusion

The $PVTx$ properties for the binary R-134a + R-290 mixtures have been measured by the constant-mass method coupled with expansion procedures at temperatures from 312 K to 400 K, pressures up to 6.1 MPa, and densities up to $196 \text{ kg} \cdot \text{m}^{-3}$, respectively. We have also determined the dew-point pressures and saturated-vapor densities for the binary R-134a + R-290 system.

Acknowledgements

We are indebted to the National Research Laboratory of Metrology, Tsukuba, for the calibration of the platinum resistance thermometer.

Literature Cited

- (1) Sato, T.; Kiyoura, H.; Sato, H.; Watanabe, K. Measurements of PVT_x properties of refrigerant mixture HFC-32 + HFC-125 in the gaseous phase. *Int. J. Thermophys*, **1996**, *17*, 43-54.
- (2) Kiyoura, H.; Takebe, J.; Uchida, H.; Sato, H.; Watanabe, K. PVT_x properties of difluoroethane + pentafluoroethane (R-32 + R-125) and difluoroethane + pentafluoroethane + 1,1,1,2-tetrafluoroethane (R-32 + R-125 + R-134a). *J. Chem. Eng. Data*, **1996**, *41*, 1409-1413.
- (3) Uchida, H.; Sato, H.; Watanabe, K. Measurements of gaseous PVT_x properties and saturated vapor densities of refrigerant mixture R-125 + R-143a. *Int. J. Thermophys*, **1999**, *20*, 97-106
- (4) Mizote, A.; Sato, H.; Watanabe, K. Measurements of PVT_x properties and saturation properties for the binary R-32/143a system. to appear in *Proc. of the 20th Int. Cong. of Refrig*, **1999**, Sydney, Australia.
- (5) Piao, C-C.; Sato, H.; Watanabe, K. An experimental study for PVT properties of CFC alternative refrigerant 1,1,1,2-tetrafluoroethane (R-134a). *ASHRAE. Trans*, **1990**, *96*, 132-140.
- (6) Aoyama, H.; Kishizawa, G.; Sato, H.; Watanabe, K. Vapor-liquid coexistence curve in the critical region and the critical temperatures and densities of 1,1,1,2-tetrafluoroethane (R-134a), 1,1,1-trifluoroethane (R-143a), and 1,1,1,2,3,3-hexafluoropropane (R-236ea). *J. Chem. Eng. Data*, **1995**, *41*, 1046-1051
- (7) Miyamoto, H.; Watanabe, K. A thermodynamic property model for fluid-phase

propane. paper submitted to *Int. J. Thermophys*, **2000**.

- (8) Holcomb, C. D.; Magee, J. W.; Scott, J. L.; Outcalt, S. L.; Haynes, W. M. Selected thermodynamic properties for mixtures of R-32, R-125, R-134A, R-143A, R-41, R-290 and R-744. *NIST technical note 1397*, **1997**.

Table 1. Experimental Results for the Binary R-134a (1) + R-290 (2) System

T/K	P/MPa	$\bullet / \text{kg} \bullet \text{m}^{-3}$	T/K	P/MPa	$\bullet / \text{kg} \bullet \text{m}^{-3}$
$x_1 = 0.25$			340.000	2.5479	99.186
352.000	3.7101	195.966	350.000	2.7152	99.139
353.000	3.7820	195.956	360.000	2.8778	99.091
355.000	3.9153	195.936	370.000	3.0363	99.044
356.000	3.9782	195.926	380.000	3.1909	98.995
357.000	4.0340	195.916	390.000	3.3417	98.947
357.500	4.0564	195.912	400.000	3.4914	98.898
358.000	4.0875	195.907	319.000	1.8870	81.748
359.000	4.1394	195.897	320.000	1.9265	81.744
360.000	4.1880	195.892	321.000	1.9686	81.740
361.000	4.2379	195.878	321.500	1.9860	81.738
365.000	4.4439	195.839	322.000	2.0019	81.737
370.000	4.6924	195.790	323.000	2.0266	81.733
380.000	5.1797	195.691	324.000	2.0401	81.729
390.000	5.6584	195.592	326.000	2.0700	81.721
400.000	6.1302	195.493	330.000	2.1258	81.706
345.000	3.2455	161.412	340.000	2.2600	81.668
347.000	3.3690	161.396	350.000	2.3896	81.629
349.000	3.4950	161.380	360.000	2.5189	81.591
351.000	3.6240	161.364	370.000	2.6428	81.551
352.000	3.6850	161.356	380.000	2.7641	81.512
352.500	3.7091	161.352	390.000	2.8863	81.472
353.000	3.7311	161.348	400.000	3.0046	81.432
354.000	3.7729	161.340	312.000	1.5973	67.331
355.000	3.8139	161.332	314.000	1.6604	67.325
357.000	3.8954	161.316	315.000	1.6901	67.322
360.000	4.0156	161.292	315.500	1.7022	67.320
370.000	4.4050	161.213	316.000	1.7178	67.319
380.000	4.7826	161.133	317.000	1.7257	67.316
390.000	5.1529	161.052	318.000	1.7401	67.313
400.000	5.5532	160.972	320.000	1.7617	67.306
$x_1 = 0.50$			330.000	1.8708	67.275
318.000	1.8597	99.289	340.000	1.9757	67.244
319.000	1.8991	99.284	350.000	2.0770	67.212
320.000	1.9441	99.280	360.000	2.1823	67.180
321.000	1.9879	99.275	370.000	2.2800	67.148
322.000	2.0282	99.270	380.000	2.3764	67.116
323.000	2.0709	99.265	390.000	2.4534	67.083
324.000	2.1188	99.261	400.000	2.5353	67.050
330.000	2.3663	99.232			

**Table 2. Dew-point Pressures and Saturated Vapor Densities
for the Binary R-134a (1) + R-290 (2) System**

T/ K	P/ MPa	$\rho / \text{kg} \cdot \text{m}^{-3}$
$x_1 = 0.60$		
329.000	2.2362	106.840
330.000	2.2806	106.835
331.000	2.3201	106.830
331.500	2.3432	106.828
332.000	2.3645	106.825
332.500	2.3789	106.823
333.000	2.3884	106.820
334.000	2.4094	106.815
335.000	2.4281	106.810
337.000	2.4634	106.800
340.000	2.5162	106.785
350.000	2.6869	106.734
360.000	2.8514	106.683
370.000	3.0119	106.632
380.000	3.1691	106.580
390.000	3.3239	106.528
400.000	3.4766	106.475
$x_1 = 0.78$		
329.000	1.9067	98.091
330.000	1.9464	98.087
331.000	1.9871	98.082
332.000	2.0273	98.078
332.500	2.0414	98.075
333.000	2.0566	98.073
334.000	2.0728	98.068
335.000	2.0875	98.064
336.000	2.1018	98.059
338.000	2.1296	98.050
340.000	2.1553	98.041
350.000	2.2923	97.995
360.000	2.4229	97.948
370.000	2.5500	97.901
380.000	2.6748	97.854
390.000	2.7973	97.806
400.000	2.9180	97.758

Figure Captions

Figure 1. Experimental apparatus: (A) sample cell; (B) expansion cell; (C) vacuum pump; (D) main heater; (E) sub heater; (F) cooler; (G) platinum resistance thermometer; (H) thermometer bridge; (I) PID controller; (J) DC power supply; (J1,J2) joints; (K) stirrer; (L) thermostated fluid bath; (M) differential pressure detector; (N) tester; (O) nitrogen cylinder; (P) precise pressure controller; (Q) digital quartz pressure transducer; (R) digital quartz pressure computer; (V1-V10) valves.

Figure 2. Distribution of PVT_x property measurements for the R-134a (1) + R-290 (2) system on a pressure-temperature plane: \diamond , $x_1 = 0.25$; \circ , $x_1 = 0.50$; Δ , $x_1 = 0.60$; \square , $x_1 = 0.78$; $-$, R-134a (Piao *et al.*⁵); \cdots , R-290 (Miyamoto *et al.*⁷); $+$, critical point of R-134a; \times , critical point of R-290.

Figure 3. Relative pressure deviations of experimental data from REFPROP (ver.6.01): \diamond , $x_1 = 0.25$; \circ , $x_1 = 0.50$; Δ , $x_1 = 0.60$; \square , $x_1 = 0.78$; \times , Holcomb *et al.*⁸

Figure 4. Determination of the dew point pressures and saturated vapor densities.

Figure 5. Experimental dew point pressures: \diamond , $x_1 = 0.25$; \circ , $x_1 = 0.50$; Δ , $x_1 = 0.60$; \square , $x_1 = 0.78$; $-$, R-134a (Piao *et al.*⁵); \cdots , R-290 (Miyamoto *et al.*⁷); $+$, critical point of R-134a; \times , critical point of R-290.

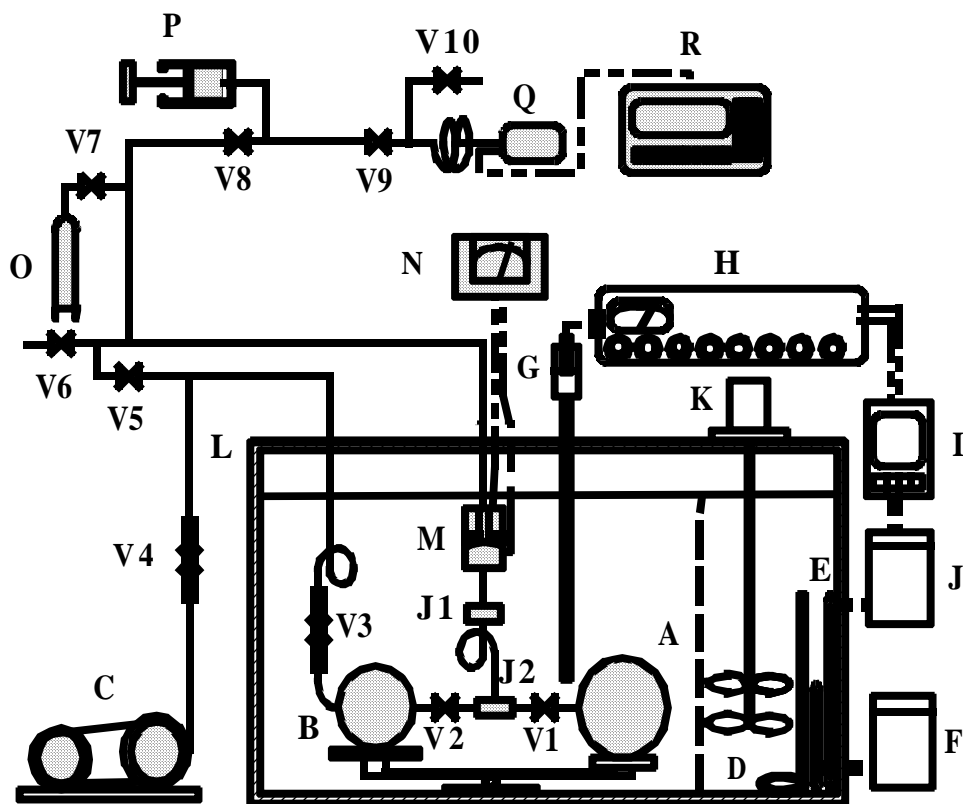


Figure 1. Experimental apparatus: (A) sample cell; (B) expansion cell; (C) vacuum pump; (D) main heater; (E) sub heater; (F) cooler; (G) platinum resistance thermometer; (H) thermometer bridge; (I) PID controller; (J) DC power supply; (J1, J2) joints; (K) stirrer; (L) thermostated fluid bath; (M) differential pressure detector; (N) tester; (O) nitrogen cylinder; (P) precise pressure controller; (Q) digital quartz pressure transducer; (R) digital quartz pressure computer; (V1-V10) valves.

Naganuma *et al.*

